IMPACT OF IMPURITY SEEDING ON PEDESTAL STRUCTURE IN ASDEX UPGRADE AND ALCATOR C-MOD

M.G. DUNNE, M. CAVEDON, T. PÜTTERICH, M. WISCHMEIER, E. WOLFRUM
Max-Planck Institute for Plasma Physics,
Boltzmannstr. 2, 85748 Garching, Germany

J.W. HUGHES, B. LABOMBARD, D. BRUNNER, A.Q. KUANG, B. MUMGAARD
Plasma Science and Fusion Center,
Massachusetts Institute of Technology, Cambridge, Massachusetts 02139, USA

M.L. REINKE
Oak Ridge National Laboratory,
1 Bethel Valley Road, Oak Ridge, Tennessee 37830, USA

L. FRASSINETTI
KTH Royal Institute of Technology,
Stockholm, Sweden

B. LIPSCHULTZ
York Plasma Institute,
Department of Physics, University of York, York YO105DD, United Kingdom

F. REIMOLD
Max-Planck Institute for Plasma Physics,
Wendelsteinstr. 1, 17491, Greifswald, Germany

The Alcator C-Mod Team

The ASDEX Upgrade Team
See the author list of "A. Kallenbach et al., Nuclear Fusion 57 102015 (2017)"

The EUROfusion MST1 Team
See the author list of "H. Meyer et al. Nuclear Fusion 57 102014 (2017)"

Email of corresponding author: mike.dunne@ipp.mpg.de

Abstract

A comparison of data sets on ASDEX Upgrade (AUG) and Alcator C-Mod is presented. Global confinement data on both machines show a dependence of the normalised confinement time on the pedestal top pressure, with overlaps of both parameters (albeit not simultaneously). The main actuator on the pedestal performance in both cases is the location of the peak edge density gradient, which has previously been shown to impact pedestal stability on several machines. The two data sets differ in that the appearance and density in the high-field side high density (HFSHD) in AUG causes the density profile to shift outwards, while in C-Mod it appears to have no effect. This is echoed in a higher current, higher density AUG discharge, indicating a limit to the ability of the HFSHD to effect changes in confinement. However, the degradation of pedestal pressure in C-Mod at higher seeding levels demonstrates that the density profile location is still an important parameter for stability, even in ELM-free discharges without the presence of a HFSHD feature.

1. INTRODUCTION

Tokamak experiments with metal walls face more challenging operational conditions compared to machines with carbon walls. Notably, the requirement to avoid the build-up of high-Z impurities places requirements on pedestal impurity transport, which translates into main-ion fuelling rates on AUG and JET to ensure high ELM frequencies. The latter criterion has, until recently, restricted operation on those devices to high density. High main-ion fuelling rates are often, although not always, connected with reduced confinement and pedestal height when compared to lower density (or fuelling rate) operation or similar discharges in the corresponding carbon walled devices.
Recent JET and AUG experiments focused on the use of impurity seeding, specifically nitrogen seeding, to improve confinement and reduce the heat load on divertor components[1, 2]. Most of the experiments combining global performance and pedestal structure studies have been limited to lower levels of nitrogen seeding, bringing the outer divertor to a high recycing or partially detached state. While the lower levels of impurity seeding are sufficient for present day machines, and perhaps even ITER, operation of a fusion power plant with solid walls

will only be possible with divertor plasma in the pronounced detachment state. Even plasmas run during the upcoming JET-DT campaign will require heat load mitigation and the use of nitrogen will not be possible. It is thus of interest to explore the impact of the scrape-off layer and divertor plasmas on the confined plasma in a range of conditions, including different impurity species. Such experiments have been carried out on ASDEX Upgrade (AUG) and Alcator C-Mod and are presented in this contribution.

The next section outlines possible SOL-pedestal interaction mechanisms. Section 3 describes the principle datasets from both machines, and the techniques used to ascertain the pedestal and SOL characteristics. Section 4 examines smaller data sets outside of the main AUG database which show behaviour more similar to the C-Mod data set. The summary and conclusions, as well as an outlook for future work, are contained in section 5.

2. SOL-PEDESTAL INTERACTIONS

An emerging view on many devices is that a shift of the location of the maximum density gradient (henceforth referred to as the location of the density profile, as it is typically close to the center of the pedestal as fitted by a modified hyperbolic tangent function) relative to some reference position, typically defined with low or zero applied fuelling or impurity seeding, can significantly affect the pedestal top pressure. This has been shown for AUG[3], C-Mod[4, 5], DIII-D[6], JET[7], and NSTX[8], and an overview from several machines is given in [9]. The effects range from either an increase in global confinement and pedestal top pressure relative to the reference case, or a confinement degradation. Confinement improvement has been observed in low collisionality discharges in DIII-D and NSTX with the application of lithium seeding, which acts to shift the density profile inwards. A reduction of the pedestal pressure is observed in highly fuelled discharges in AUG and JET, correlated with an outward shift of the density profile. A reversal of the confinement degradation on AUG is possible with the application of nitrogen seeding, which shifts the profile inwards towards its original location.

Although the movement of the density profile is common across these devices and experiments, the origin of the shift can be different. In the NSTX example, the main chamber recycling is significantly reduced by the application of Li-seeding, resulting in the inward profile shift. Li-seeding has a different effect in DIII-D where it excites a pre-existing mode in the density pedestal, causing a local flattening of the density profile and effecting an inward shift. In Alcator C-Mod, two separate experiments have shown profile shifts; main ion fuelling during the H-mode phase was shown to shift the profile outwards, while LHRF focussed on the SOL could reverse the fuelling degradetion of the pedestal by effecting an inward shift.

At AUG, a SOL feature appears in most H-mode conditions with sufficient main ion fuelling and heating power known as the high field side high density (HFSHD)[10]. This feature is localised to the HFS SOL, extends from the divertor to at least the midplane, and has a density approximately one order of magnitude higher than typical separatrix densities. Modelled HFS profiles show a separatrix density of 4×10^{19} m^{-3}, or twice the value of the separatrix density at the LFS, and an inverted midplane profile[11]. This indicates the possibility of diffusive fuelling from the HFSHD feature, adjusting the separatrix density and hence potentially leading to the outward profile shift observed with increased deuterium fuelling. The density and poloidal extent of the HFSHD can be reduced with impurity seeding, leading to the shift of the density profile back towards its original position and the concomitant pedestal pressure recovery.

After the discovery and modelling of the HFSHD on AUG, interest was also sparked on Alcator C-Mod to check for the HFSHD feature and any potential effects on confinement. The analysis of divertor and SOL plasmas will be presented in a separate contribution, and the analysis of the pedestal will be presented here and compared to the AUG observations.

3. EXPERIMENT DESCRIPTION

The data set from AUG has been described in detail in [3, 12]. It consists of Type-I ELMing H-mode plasmas with 1 MA plasma current, -2.5 T field (resulting in a q_{95} of 4) at low triangularity. A range of heating powers (5-15 MW of combined NBI, ECRH, and ICRF), fuelling levels, and impurity seeding levels results in a range of pedestal top temperature between 400 and 1100 eV and confinement times normalised to the ITER-98,y2 scaling $H_{98,y2}$ between 0.8 and 1.2. The C-Mod data set, described in [13, 14] consists of EDA H-modes at 800 kA and 5.4 T with a small variation in applied ICRF heating power between 2.8 and 3.5 MW. Pedestal temperatures vary between 200 and 600 eV, and $H_{98,y2}$ between 0.6 and 0.9. Readers should note that H-factors on C-Mod are artificially low due to the density dependence in the ITER-98,y2 scaling which is typically not reproduced in single

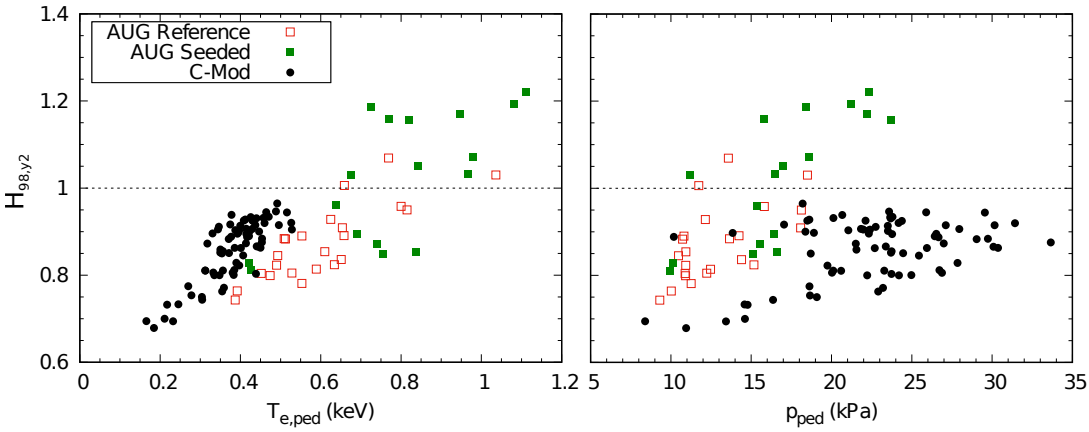

FIG. 1. $H_{98,y2}$ as a function of pedestal top temperature (left) and pressure (right) for both AUG (red, green) and C-Mod (black).

machine studies. The pedestal density in these C-Mod discharges is around 2×10^{20} m^{-3}. Previous confinement studies on C-Mod have shown that the confinement time scales strongly with heating power[15].

The dependence of the normalised confinement time in both machines on pedestal temperature (left) and pressure (right) is shown in figure 1. C-Mod data are shown as black dots, while the AUG data sets are colour coded by unseeded (red) and nitrogen seeded (green) squares. The C-Mod data are not divided into seeded and unseeded as a continuous scan from zero applied impurity level (not accounting for intrinsic impurities) to very high seeding rates was performed so the data set is in a state of constant transition. The electron temperature and density on both machines are measured by Thomson Scattering, with the AUG measurements augmented by ECE (T_e) and lithium beam and DCN interferometry (n_e) diagnostics. The ion temperature is measured on AUG via charge exchange recombination spectroscopy, which is also used to measure the impurity density to allow the correct ion pressure (accounting for impurity content) to be calculated. For C-Mod, these measurements are not regularly available, so the ion pressure has been assumed to be the same as the electron pressure for the analysis in this paper.

The low temperature, high density C-Mod pedestal results in lower H-factors, despite the higher average pedestal pressure when compared to AUG. The global confinement on both machines is strongly influenced by the pedestal behaviour, as shown in previous studies. This motivates a detailed look at the pedestal composition on both devices to compare the changes effected by main ion fuelling and impurity seeding on pedestal stability. The AUG data have already been shown to be limited by peeling-ballooning modes, facilitating the use of predictive pedestal models to understand the physics behind changes in pedestal stability. The C-Mod pedestals, on the other hand, are not limited by peeling-ballooning modes, but by some other instability. A comparison between thet two devices is still interesting, however, since the C-Mod pedestal has previously been shown to vary in a ballooning-like fashion[16]. Therefore, while any predictive modelling will not deliver accurate pedestal top values, trends may give a good indication of how the pedestal pressure should react to, for example, a radial shift of the density profile.

An overview of the pedestal parameters is shown in figure 2 for both machines. Readers will observe the different axis ranges for both subfigures, with C-Mod pedestals occurring at higher density and lower temperature, but similar overall electron pressure. The range of pressures in the AUG case spans a factor of 3, while in the C-Mod case, this is around a factor of 2 and shifted to slightly higher pressures.

While the AUG pedestal density is relatively constant in this data set, the C-Mod density spans a large range. Conversely, the AUG pedestal top temperature is responsible for the majority of the increase in pedestal pressure in response to impurity seeding. Of more interest in the comparison between the two machines are the causes of the spread of the pedestal height. In the case of the AUG data set, this has previously been shown to be linked with the separatrix density and, hence, the location of the density profile[3]. As mentioned above, the separatrix density is affected by the presence of the HFSHD, the density and poloidal extent of which can be varied by different fuelling and seeding rates, and heating powers. Figure 3 shows the total pedestal pressure for AUG and C-Mod as a function of two parameters. In the left subfigures, pedestal pressure is plotted against Z_{eff} for AUG and the intensity of a nitrogen-vii line from spectroscopic measurements for C-Mod, showing different trends for both cases. In the AUG case, pedestal pressure continuously increases as impurity seeding is applied, owing to the reduction of the HFSHD. In the C-Mod case, the pedestal pressure is initially unaffected by the impurity seeding

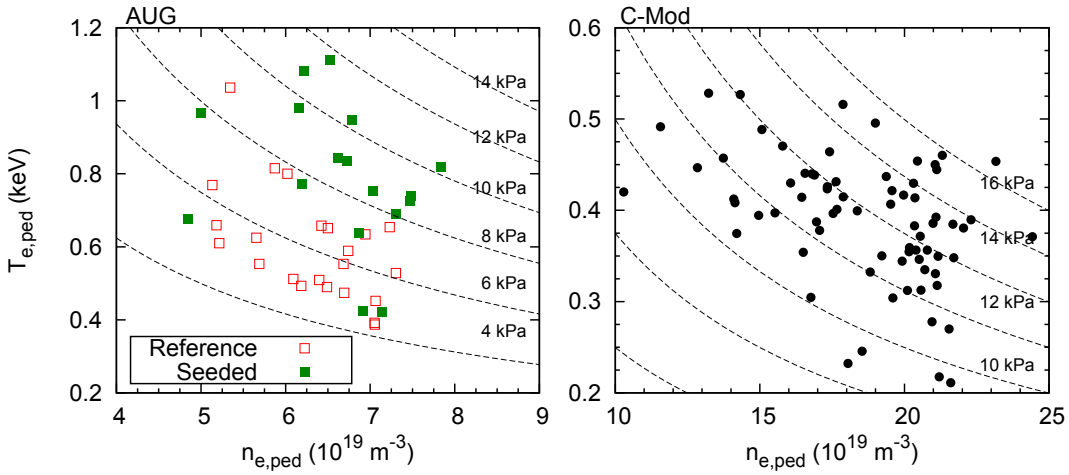

FIG. 2. Pedestal top T_e vs n_e plots for AUG (left) and C-Mod (right). Reference (red) and seeded (green) points are marked for AUG. Even at high densities, high pedestal top temperatures and electron pressures can be obtained in both machines.

and later falls off once a critical threshold has been reached, and both Z_{eff} and global radiated power are noticeably increased.

It should be noted at this point that both data sets cover a different range in divertor properties. The AUG data set consists of plasmas with an attached to highly recycling outer divertor, while the C-Mod data cover a range up to a completely detached outer divertor; the outer divertor progresses from partially to fully detached around the roll-over point in the dependence of the pedestal top on the N_{vii} emission, indicating a negative impact of deep detachement on confinement in these plasmas. In terms of the divertor plasma, the AUG data set overlaps with the low seeding part of the C-Mod data set (at its highest pedestal pressure). This means that a direct comparison of the impact of detachment on pedestal pressure is not possible at the moment, though an AUG data set which covers the transition from partial to full detachment is being constructed at the moment.

In the low seeding cases from C-Mod, a high density feature is observed in the HFS-SOL, but it is not yet clear if this is the same as the HFSHD on AUG. This high density, measured by Stark broadening, does decrease with increasing impurity seeding, which is phenomenologically similar to the effect of impurity seeding on the AUG HFSHD, and it also appears to reach outside of the HFS divertor region. Despite these similarities, the high density feature in C-Mod appears to have no impact on the separatrix density, the location of the density profile, or confinement. What is common to both the AUG and C-Mod datasets, however, is the correlation between the pedestal top pressure and the location of the density gradient, shown in the right subfigures of figure 3. The highest pedestal pressure is obtained when the density profile is furthest inwards and steadily decays as it moves outwards. In the C-Mod case, this happens as the divertor progresses into deep detachment and the detachment front moves away from the target plates and towards the x-point, as determined from the radiation intensity measured by bolometer chords. Two questions now arise: why does the high density feature not affect the separatrix density and profile shift in the C-Mod discharges, and what causes the later outward profile shift which results in confinement degradation?

One possible answer for the first question is that the natural separatrix density on C-Mod is too high to be affected by the proposed diffusive fuelling of a HFSHD-like feature. While a broader C-Mod dataset[15] has shown a correlation of pedestal top pressure with the separatrix density (normalised to the pedestal density), this variation in the separatrix density was achieved passively. The main-chamber was boronised and repeated discharges on the following day led to a decrease in PFC outgassing during OCRF operation and, hence, a decrease in $n_{e,sep}/n_{e,ped}$. The modelling for AUG shows a HFS separatrix density of 4×10^{19} m^{-3} when the HFSHD is present, which is similar to the standard C-Mod separatrix density. If the density in the HFSHD is also similar, then there may not be enough of a gradient to create a diffusive fuelling effect. Figure 4 shows the pedestal pressure on both machines as a function of the separatrix density normalised to the pedestal top density. The highest confinement typically observed in a number of machines occurs at separatrix densities of ~$0.25 - 0.3\ n_{e,ped}$. In both devices, the highest confinement is observed at the lowest normalised separatrix density; this has already been shown for C-Mod in a wide database[15], and a similar plot with only the separatrix density has been shown for AUG[3]. The minimum

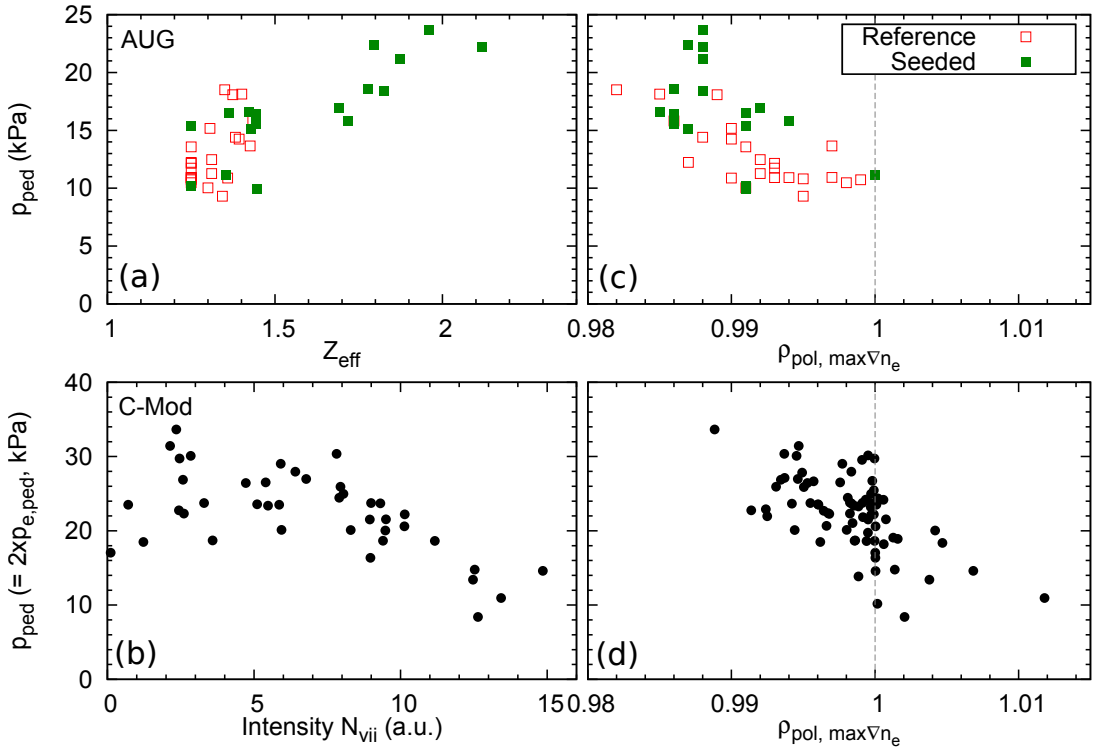

FIG. 3. Pedestal top pressure in AUG (top) and C-Mod (bottom) as a function of impurity content (left) and location of the density profile (right). While both machines show different trends of pedestal pressure with impurity content, the mechanism affecting the attainable pressure appears to be linked to the location of the density profile.

separatrix value in C-Mod is approximately 40% of the pedestal top density, which overlaps with the bulk of the highest pedestal pressure data on AUG. Since this density corresponds to an unnormalised separatrix density of around $7\times10^{19}m^{-3}$, it is entirely possible that the HFSHD as observed on AUG would not affect the separatrix density. A scenario with high absolute separatrix density also exists on AUG; the ITER baseline scenario at high triangularity, which we analyse in the following section.

4. IMPURITY SEEDING IN HIGH TRIANGULARITY SCENARIOS ON AUG

The ITER baseline (BL) impurity seeding studies are described in detail in a separate contribution at this conference[17]. The scenario has a higher plasma current (1.2 MA) and lower field (-2.0 T) resulting in a q_{95} of around 3. A general observation is that the desired normalised confinement of 1 is only attainable in discharges with a β_N of ~2.2, which is significantly higher than the target value of 1.8. Nitrogen seeding has been added to high triangularity ITER-BL plasmas with $H_{98,y2}$~1 and β_N~2.2 in an attempt to improve performance, as observed in the AUG experiments described above. The HFSHD, commonly observed at the high fuelling levels typical of the AUG ITER-BL plasmas, is significantly reduced when nitrogen seeding is applied. However, no change of the stored energy (or confinement) is observed. Pedestal profiles of temperature and density from one example discharge are shown in figure 5. The temperature profiles have been aligned to 100 eV at the separatrix, as performed for all profiles on both machines in this contribution, which automatically aligns the density profiles correctly due to the use of Thomson Scattering. When nitrogen seeding is applied the electron temperature decreases while the density increases, but no significant change in the separatrix density can be observed. The location of the peak gradient is also not changed, though it does become steeper.

Why the impurity seeding does not lead to a change in confinement, or to a shift in the density profile despite the density reduction of the HFSHD is not immediately clear. However, it may be, as it appears in the C-Mod cases, that the reference scenario is not affected by the HFSHD feature. The separatrix density, while high, is approximately 1/3 of the pedestal top density in both cases, which is quite typical of high confinement plasmas in the AUG data set at lower plasma current. This may imply that the scenario simply has a naturally high separatrix density which cannot be further affected by the presence of the HFSHD. If the modelled elevated

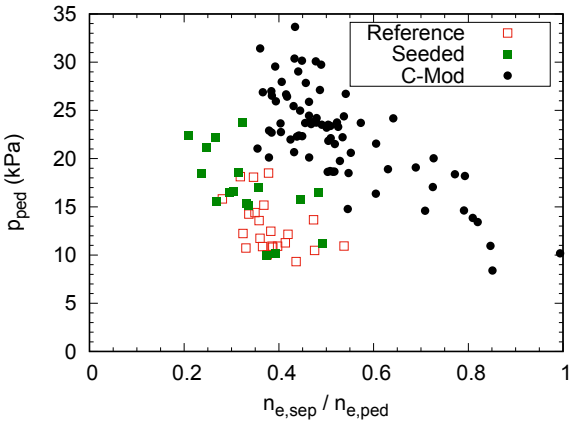

FIG. 4. Pedestal top pressure as a function of $n_{e,sep}$ normalised to $n_{e,ped}$ for both AUG and C-Mod.

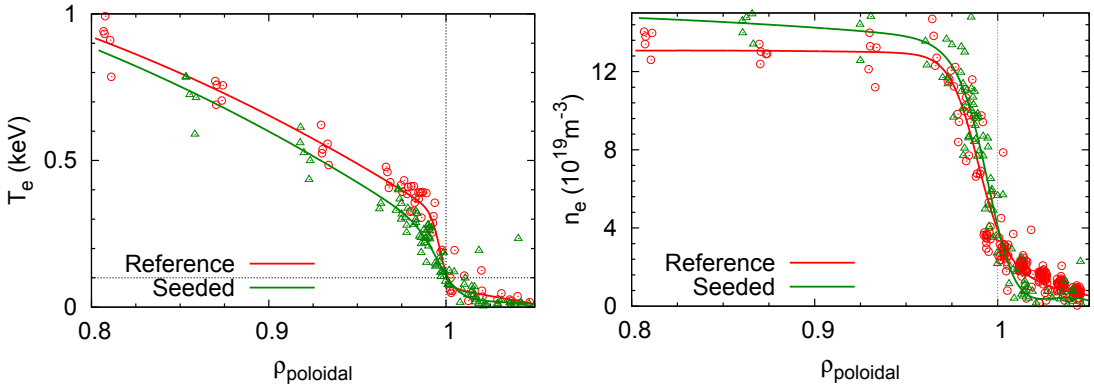

FIG. 5. Profiles of T_e (left) and n_e for the ITER BL discharge #34441 at 3.5 s (red, without nitrogen seeding) and 4.5 s (green, with nitrogen seeding). Despite changes in the pedestal top values of temperature and density, the overall pressure is not significantly affected by nitrogen seeding.

midplane separatrix density values of 4×10^{19} m^{-3}, determined for the lower plasma current, are the same for the higher current, then it can perhaps be expected that the HFSHD can no longer contribute to the proposed diffusive fuelling mechanism. More detailed analysis of the characteristics of the HFSHD at the elevated plasma current of 1.2 MA should be carried out to diagnose its scaling with power; since the density of the HFSHD increases with heating power, it may be possible to degrade the pedestal pressure through this mechanism only at higher heating power at 1.2 MA.

5. CONCLUSIONS AND OUTLOOK

A comparison of pedestal data sets from ASDEX Upgrade and Alcator C-Mod H-modes has been presented. The global confinement on both machines follows the behaviour of the pedestal, as expected. While the AUG data are mostly at a lower absolute density and higher temperature, there is considerable overlap in the pedestal pressure on both machines. In both devices, the attainable pedestal top pressure is correlated with the location of the peak edge density gradient. The mechanism by which the density gradient can be shifted is different in both devices, however. In the presented operational range in AUG, the HFSHD is responsible for an outward shift of the density profile. Impurity seeding reduces the poloidal extent and density in the HFSHD, allowing the profile to shift radially inwards. In C-Mod, the confinement and pedestal pressure do not appear to be affected by the presence of high density in the inner divertor (a difinitive statement referring to this as the same structure as the AUG and JET HFSHD cannot be made at this point), which reduces in density as impurity seeding is applied. However, once the outer divertor progresses from partially towards fully detached, the density profile starts to move outwards and confinement degrades.

This comparison highlights two important points. Firstly, the HFSHD may not always be an issue for confinement degradation, and its removal does not necessarily result in confinement improvement, especially at naturally high

separatrix densities. This has also been shown for an AUG ITER-BL plasma at high triangularity, where the confinement is not significantly affected by nitrogen seeding, although the ELM behaviour does change. Secondly, this comparison also highlights that an outward density profile shift can have other causes than just the HFSHD, particularly around the onset of detachment. This is interesting for future machines, as it will be a favoured operational regime in order to protect the divertor. In this regard Alcator C-Mod offers a unique possibility to asses the impact of this transition on the pedestal as the nature of the instability does not change at the higher density and lower temperature operation of detached plasmas; most AUG plasmas which approach detachment change the ELM type from Type-I to Type-III (or some other small ELM type), which may have additional unknown effects on the allowable pedestal pressure.
Nevertheless, extending the comparison between the two machines by adding AUG data points with higher levels of imputrity seeding which progress further towards detachment is a priority. In addition, further analysis of additional ITER-BL plasmas, particularly those with lower confinement, could provide more insight into the range of impact the HFSHD can have on higher density plasmas and help inform the comparison of the two machines.

Acknowledgements

This work has been carried out within the framework of the EUROfusion Consortium and has received funding from the Euratom research and training programme 2014-2018 under grant agreement No. 633053. The views and opinions expressed herein do not necessarily reflect those of the European Commission. Supported by U.S. Department of Energy awards DE-AC05-00OR22725, DE-FC02-99ER54512, DE-SC0014264 using Alcator C-Mod, a DOE Office of Science User Facility.

REFERENCES

[1] C Giroud, et al. *Plasma Physics and Controlled Fusion*, 57(3), 2015.

[2] M.G. Dunne, et al. *Plasma Phys. Control. Control. Fusion*, 59(3), 2017.

[3] M.G. Dunne, et al. *Plasma Physics and Controlled Fusion*, 59(1), 2017.

[4] J W Hughes, et al. *Nuclear Fusion*, 47(8), 2007.

[5] J L Terry, et al. *Physics of Plasmas*, 22(5), 2015.

[6] T.H. Osborne, et al. *Nuclear Fusion*, 55(6), 2015.

[7] E. Stefanikova, et al. *Nuclear Fusion*, 58(5), 2018.

[8] R. Maingi, et al. *Physical Review Letters*, 107(14), 2011.

[9] E. Wolfrum, et al. *Nuclear Materials and Energy*, 12, 2017.

[10] S. Potzel, et al. *42nd European Physical Society Conference on Plasma Physics, EPS 2015*, 2015.

[11] F. Reimold, et al. *Nuclear Materials and Energy*, 12, 2017.

[12] M.G. Dunne. *Nuclear Fusion*, 57(2), 2017.

[13] J D Lore, et al. *Physics of Plasmas*, 22, 2015.

[14] M L Reinke, et al. *Plasma Physics and Controlled Fusion*, 59, 2017.

[15] J.W. Hughes, et al. *Nuclear Fusion*, 51(8), 2011.

[16] J. W. Hughes, et al. *Physics of Plasmas*, 9(7), 2002.

[17] T. Pütterich. EX/P8-4. In *IAEA FEC*, 2018.